EEET ECOLOGICAL ENGINEERING & ENVIRONMENTAL TECHNOLOGY

*Ecological Engineering & Environmental Technology* 2024, 25(9), 1–12
https://doi.org/10.12912/27197050/189237
ISSN 2299–8993, License CC-BY 4.0

Received: 2024.04.26
Accepted: 2024.07.10
Published: 2024.08.01

# Study of the Impact of Drip Irrigation on Soil Salinization in the Al Haouz and Kelaa des Sraghna Region

Imane El Kihal[1*], Ahmed Algouti[1], Abdellah Algouti[1], Abdelhalim Tabit[1], Naji Jdaba[1], Imane Toudamrini[1], Khadija Lamrani [1], Kaouthar Majdouli[1], Jaouad Aadaj[1], Rachid Es-Sadiq[1]

[1] Laboratory Sedimentary Basins Geology of Moroccan, "2GRNT" Geology Department, Faculty of Science Semlalia, University Cadi Ayyad, BP 2390, 40000, Marrakech, Morocco

* Corresponding author's e-mail: i.elkihal.ced@uca.ac.ma

## ABSTRACT

The El Haouz and El Kelaa Des Sraghna region is renowned for its agriculture, but is facing problems of salinisation due to its arid climate and unfavourable weather conditions. To remedy this, localised irrigation systems have been introduced to provide water for crops and improve yields. This study examines the impact of these irrigation systems on soil salinity in the region by comparing upstream and downstream areas. Using remote sensing techniques, we identify areas at risk of high salinity and collect soil samples for physical and chemical analysis in the field. These analyses enable us to monitor changes in salinisation and assess the effectiveness of localised irrigation in the areas concerned. Our results reveal two distinct zones in the region: an upstream zone with low salinity, with electrical conductivity ranging from 66 µS/cm to 345 µS/cm, and a downstream zone with higher salinity, with electrical conductivity ranging from 228 µS/cm to 1.075 µS/cm, attributed to the use of localised irrigation for crops. The remote sensing maps anticipated this difference, which was confirmed by the field analyses.

**Keywords:** GIS, salinization, localized irrigation, soil quality, arid climate, agricultural productivity.

## INTRODUCTION

In arid and semi-arid regions, the growing demand for irrigation water represents a major challenge for agriculture. Water is the factor that limits agricultural production (Cattiveli et al., 2008). Given the increasing scarcity of water, the agricultural sector (which mobilises more than 80% of water resources, Belghiti (2012) is called upon to make good use of irrigation water by making better technical, economic and social use of this resource, and above all to preserve it for future generations (Moghli and Benjelloun, 2000).

Localised irrigation is seen as a water-efficient technique that increases yields and is often proposed as a response to major water crises (Postel, 2000; Bourzac, 2013). Agricultural management must adapt to this reality, particularly by taking salinity into account, a key factor in optimising the relationship between water requirements and agricultural production. Salinity is one of the main obstacles affecting crop yields and health (Messedi and Abdelly, 2004).

The area of land affected by salts is estimated at between 400 and 950 hectares (Massoud, 1974). In arid zones, soil salinity is a major environmental and agricultural concern (Baatour et al., 2004), mainly as a result of rapid evaporation of water from the soil and irregular and insufficient rainfall (Munns et al., 2006).

Numerous studies carried out in various parts of the world have highlighted these problems: in West Africa, for example, according to (Samba, 1998), Cheverry (1974) and Al Droub (1976) in Chad, Ndiaye (1987) and Vallès et al. (1989) in Mali, Barbiéro and Vallès (1992), Barbiéro et al. (1995) in Niger, and Loyer (1989) in Senegal. And in the Maghreb (North Africa) according to

(Bradai, 2017); Derbbah and Badraoui (2003) and Ben Abbou et al. (2014) in Morocco. The Haouz irrigated area is one of the oldest and largest in the region, and is undergoing an intensification of farming practices. Although this intensification is having a positive effect on agricultural yields, it is also having a negative impact in terms of degrading the quality of both the soil and the receiving environment, particularly the water table. Indeed, recent studies in this region have shown the existence of problems of salinity, sodification, clogging and nitric pollution of groundwater (Aniba, 1997; Id Ahmad, 1998; Rahoui et al., 1999a).

This article seeks to delve into these issues by investigating the soil salinization status in the El Haouz and Kelaa Des Sraghna regions, utilizing a combination of field observations and remote sensing techniques. Additionally, physico-chemical analyses will bolster our research efforts, with the goal of gaining a deeper understanding of the impact of localized irrigation in this area.

## METHODOLOGY

The study is conducted in the Marrakech-Safi region, located 130 km northeast of the city of Marrakech, encompassing the perimeter of the Kelaa des Sraghna province. This area extends in a north-south direction at the eastern end of the region (Figure 1).

The study focuses on 22 localities divided into two parts: the upstream Tassaout and the downstream Tassaout. Sampling sites along the Tassaout are similarly distributed, with 11 in the upstream Tassaout (Attaouia, Chaibia, etc.) before the intersection of the Tassaout River and the Lakhdar River. The other 11 sites are located after Faraita, at the downstream Tassaout (Kelaa des Sraghna, Ouled Bougrine, etc.).

### Satellite images

As part of our study, we aim to identify the similarities and disparities in salinity between the peripheral areas of the upstream Tassaout and the downstream Tassaout using SENTINEL-2 satellite imagery (Table 1).

### Vegetation index

The normalized difference vegetation index (NDVI) is among the vegetation indices used to map vegetation cover. It requires the use of a combination of different spectral bands to obtain values reflecting the proportion of vegetation present in each pixel. Its principle relies on the ability of plant chlorophyll to absorb energy in the red band and to reflect significantly in the near-infrared band. NDVI is defined by the following formula (Roy, 2008):

$$NDVI = \frac{NIR - R}{NIR + R} \quad (1)$$

This index is used to estimate vegetation cover in the upstream and downstream regions of the Tassaout, allowing us to identify areas with extensive vegetation or a high index. According to the map, the upstream region of the Tassaout near Attaouia

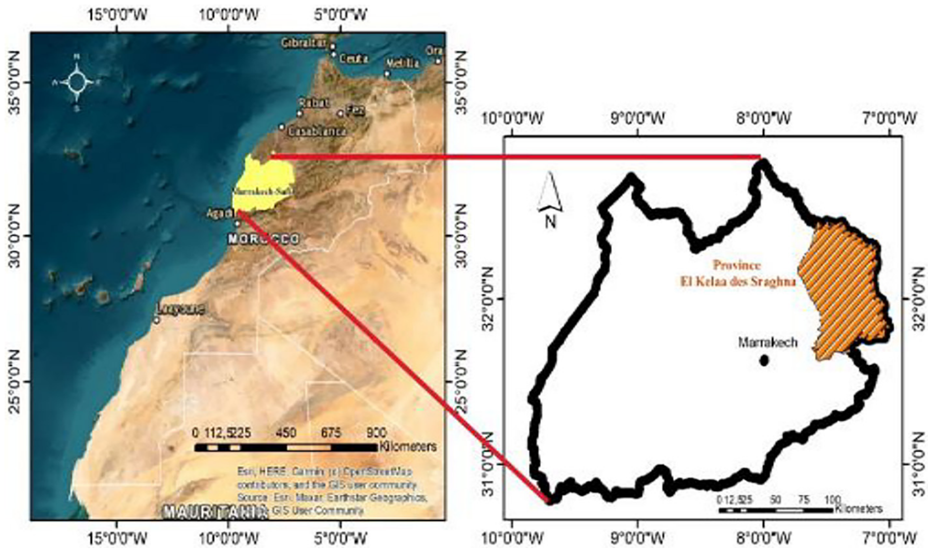


**Figure 1.** Localization of the study area

**Table 1.** The corresponding bands in SENTINEL-2 to be used are as follows

| Landsat TM | SENTINEL-2 |
|---|---|
| B1 | B2 |
| B2 | B3 |
| B3 | B4 |
| B4 | B8 |

and surrounding areas exhibit dense vegetation cover, with values ranging from 0.7 to 0.1 and high percentages (Figure 2). However, the downstream part of the Tassaout is largely characterized by values below 0, suggesting a reduced proportion of vegetation. It is interesting to note that the Kelaa des Sraghna region, although known for its significant agriculture, shows relatively low vegetation indices in the downstream part of the Tassaout.

## Salinity and brightness indexes: SI and BI

The salinity index is used to evaluate the brightness or reflectance of surfaces. These two indexes allow for the high potentiality of salinity and the localization of areas with high levels. We have calculated the salinity index (SI) as follows (Figure 3):

$$SI = \sqrt{B2 \times B4} \tag{2}$$

$$BI = \sqrt{B4 + B8} \tag{3}$$

## NDSI index

The normalized difference salinity index (NDSI) is a reliable tool for identifying potential sources of salinity on the soil surface. This index accurately locates areas of high salinity throughout the studied region and makes a significant distinction between different classes of the region, particularly those with a salinity source compared to those without (Sadiki et al., 2016). This index is calculated by the formula:

$$NDSI = \frac{Green - Red}{Green + Red} \tag{4}$$

## Fieldwork and sampling

The sampling sites were distributed according to a methodical strategy, covering both upstream and downstream areas as well as both banks of the Tassaout River. It is worth noting that the selection of stations was not arbitrary, but rather based on the presence of vegetation and irrigated perimeters. Additionally, an assessment of water

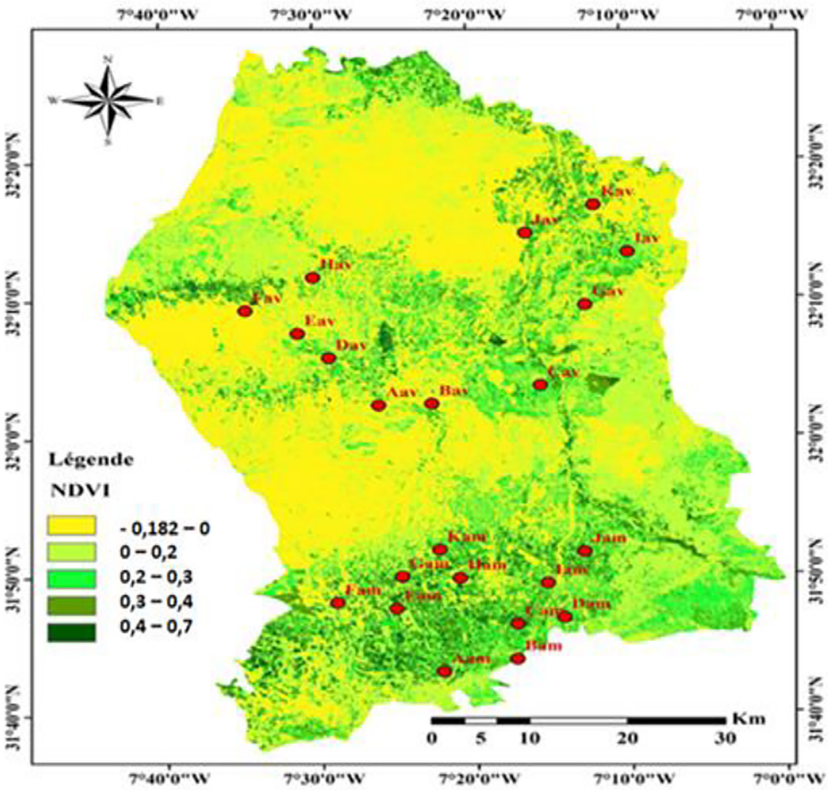


**Figure 2.** NDVI map of the study area's perimeters

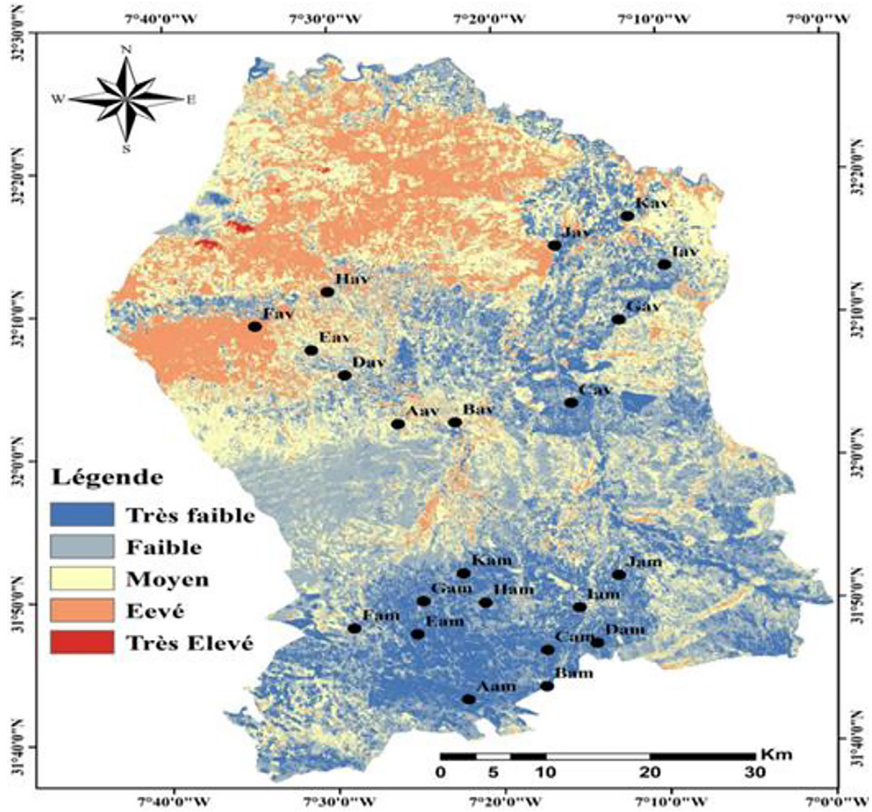


**Figure 3.** Salinity index (SI) map

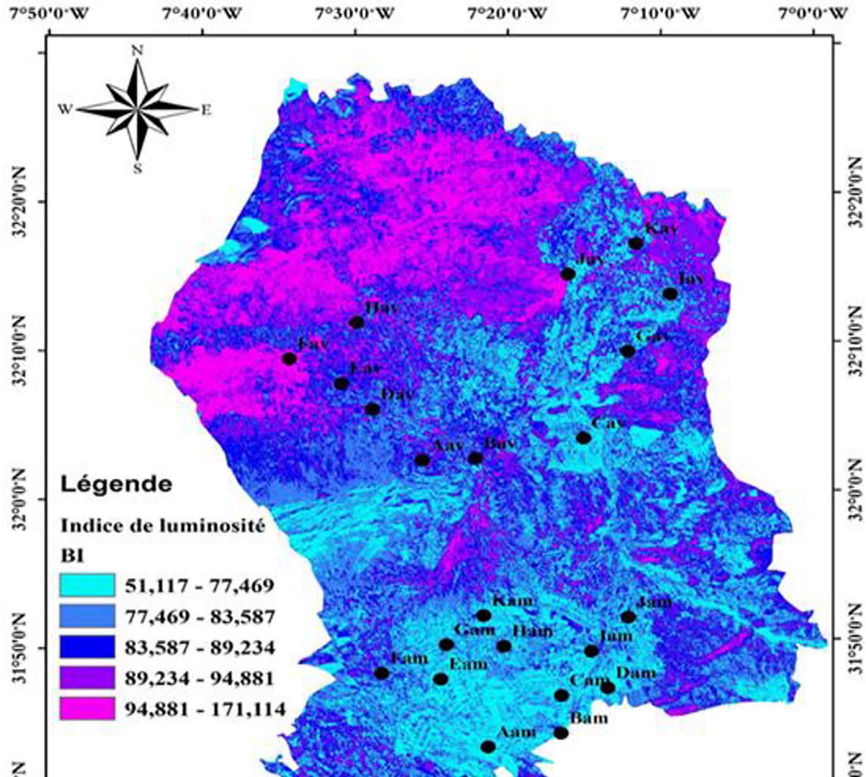


**Figure 4.** Brightness index (BI) map of the study region

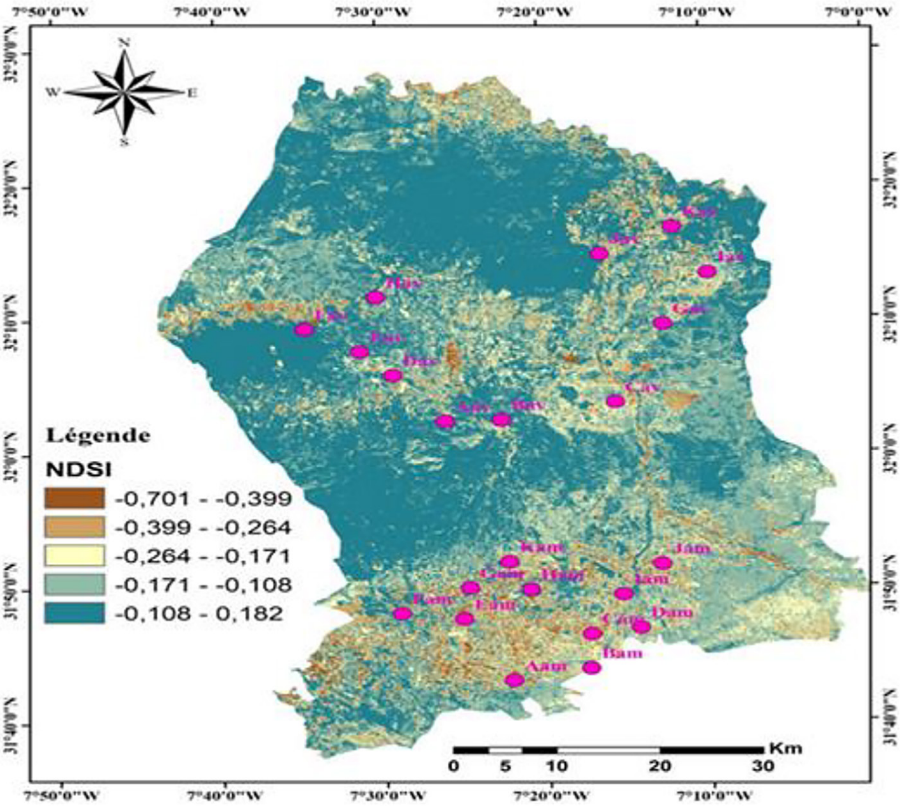


**Figure 5.** NDSI map of the study region

parameters from the wells supplying each site was conducted on-site.

### Electrical conductivity measurement

The measurement procedure begins with the calibration of the conductivity meter, following the instructions provided in the operating manual and using calibration solutions. This equipment consists of two main components: a probe for detecting the conductivity of the solution and an electronic device that displays the value of electrical conductivity (EC) (Figure 6).

### Measurement of hydrogen potential

A calibrated pH meter is used, and the value at which the device stabilizes is recorded (Figure 7).

### Temperature measurement

To ensure the accuracy of water temperature, two methods are employed during measurement. The first involves using a thermometer, while the second involves adjusting the pH meter calibration to function as a thermometer. The recorded value is the average of the two measurements (Figure 8).


**Figure 6.** Conductivity measurement

### Physicochemical analyses and laboratory work – top of form

For the analysis of physicochemical parameters of soils related to salinity and alkalinity (electrical conductivity, pH, concentration of specific ions...);

**Figure 7.** Value detected by the conductivity meter

## Chemical analyses

*Atomic absorption spectometry:*

To calculate the SAR coefficient and estimate the excess amount of potash in soil samples from the downstream and upstream Tassaout, it is essential to apply a quantitative method for specific chemical elements (K, Na, Mg, Ca). This method relies on the phenomenon of light absorption by atoms of the element of interest.

*CNHS-O analysis*

Elemental CNH-S microanalysis allows for quantifying the proportions of different elements such as carbon (C), hydrogen (H), nitrogen (N), sulfur (S), and oxygen (O) present in a sample. This method relies on redox reactions of the elements being analyzed, generating the formation of gases. These gases are then separated and analyzed using gas chromatography (Borgie, 2014).

This technique is particularly useful for determining the percentages of carbon and nitrogen, which are essential for evaluating the amount of organic matter in soil samples

**Figure 8.** Thermometer

*Laser granulometry (fine granulometry)*

The determination of soil texture in soil samples is carried out using the laser diffraction fine granulometry method, an indirect method widely used to evaluate the size distribution of pulverulent granular materials (Michel and Corard, 2006). This method provides information on the distribution of particle sizes in a sample, distinguishing between sand, silt, and clay fractions, using the phenomenon of laser light diffraction. This technique has been used for about twenty years (Duval et al., 2020). The results of soil samples are then presented in Excel spreadsheets, including quantiles, percentages of each fraction, and the grain size distribution curve (see Appendix), based on the three particle size families:

- clay: 0.1–2 µm
- silt: 2–63 µm
- sand: 63–2 mm

*Measurement of soil electrical conductivity and pH soil solution extraction*

To take measurements, a solution is prepared based on the solid state of the soil, transforming it into an electrolyte. This aqueous extraction allows for the direct measurement of the ability to conduct electrical current by the conductivity meter (Montroi, 1997). The diluted extract is formed by a ratio between the amount of soil and the amount of water used to prepare the extract, and this ratio is fixed for all samples from the downstream and upstream Tassaout.

The collected soil is dried in open air and passed through a 2 mm sieve to remove visible organic matter. Then, a solution of 50 ml of deionized water is prepared, to which 10 g of the dried and sieved soil is added. It is important to note that the ratio between water and soil is generally 1/15, meaning that the mass of water added is equivalent to five times the mass of soil (10 g) (Montroi, 1997).

## RESULTS AND DISCUSSION

### Organic matter

The CNH-S analyses of organic elements provided the percentages of carbon (C) and nitrogen (N) present in the soil samples. Taking into account the molar masses (M) of these elements, we apply the following relationship:

$$MO = \frac{M(C) \times Percentage(C)}{M(N) \times Percentage(N)} \quad (5)$$

where: $M$ – molar mass, $M(C) = 12$, $M(N) = 14$.

The results are provided in Table 2 and Table 3 for both the upstream and downstream parts of the area. According to the data, a clear distinction appears between the upstream and downstream Tassaout, with lower downstream. For example, a C/N ratio of 10 would indicate that the soil contains 10 times more carbon than nitrogen. The higher values of the ratio suggest slow mineralization of organic matter in the downstream part.

### Soil electrical conductivity and hydrogen potential

The prepared soil solutions are used to measure electrical conductivity using a conductivity meter, and the pH is measured using a pH meter

**Table 2.** Carbon and nitrogen percentages at the upstream Tassaout

| The sample | Carbon percentage (C) | Nitrogen percentage (N) | MO (C/N) |
|---|---|---|---|
| Aam | 1.728 | 0.310 | 04.78 |
| Bam | 1.515 | 0.292 | 04.44 |
| Cam | 1.948 | 0.300 | 05.56 |
| Dam | 1.711 | 0.358 | 04.09 |
| Eam | 1.769 | 0.310 | 04.89 |
| Fam | 1.645 | 0.332 | 04.24 |
| Gam | 1.895 | 0.289 | 05.62 |
| Ham | 1.638 | 0.293 | 04.79 |
| Iam | 1.530 | 0.296 | 04.43 |
| Jam | 3.339 | 0.331 | 08.64 |
| Kam | 1.173 | 0.255 | 03.94 |

**Table 3.** Carbon and nitrogen percentages at the downstream Tassaout

| The sample | Carbon percentage (C) | Nitrogen percentage (N) | MO (C/N) |
|---|---|---|---|
| Aav | 3.002 | 0.374 | 06.88 |
| Bav | 1.815 | 0.40 | 3.88 |
| Cav | 1.602 | 0.60 | 2.28 |
| Dav | 2.291 | 0.779 | 02.29 |
| Eav | 3.233 | 0.174 | 15.92 |
| Fav | 2.032 | 0.214 | 08.18 |
| Gav | 5.107 | 0.270 | 16.21 |
| Hav | 2.754 | 0.181 | 13.04 |
| Iav | 2.837 | 0.182 | 13.36 |
| Jav | 0.265 | 0.075 | 03.03 |
| Kav | 3.041 | 0.245 | 10.63 |

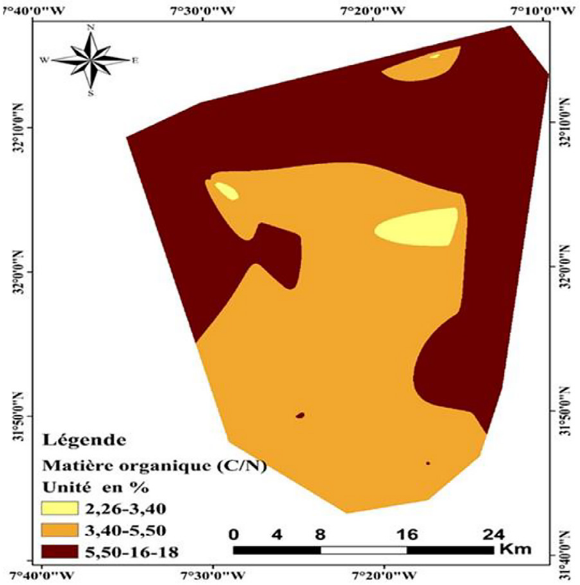


**Figure 9.** Interpolation map of organic matter data

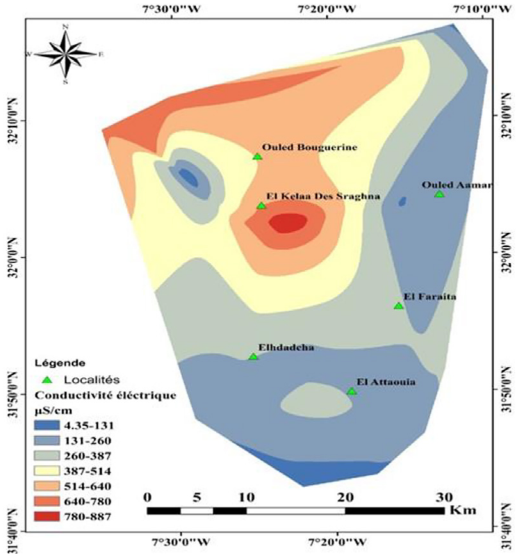


**Figure 10.** Interpolation map of electrical conductivity results

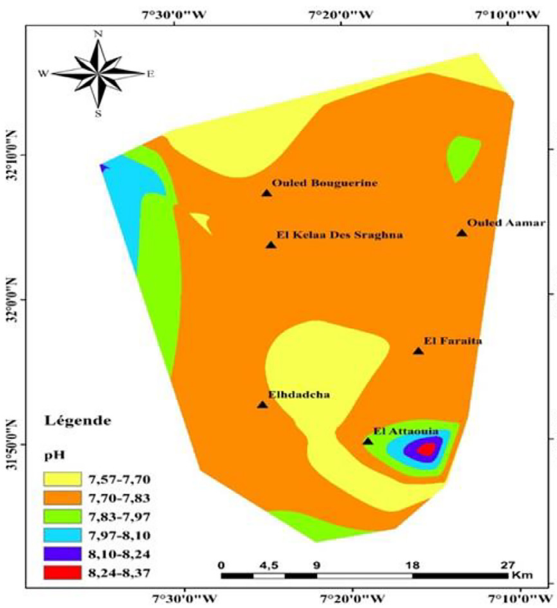


**Figure 11.** Interpolation map of hydrogen potential results

after 30 minutes of settling. The obtained values are as follows shown in Table 4 and Table 5.

The electrical conductivity from the analyses reveals a clear variation between the upstream and downstream areas, with a gradual increase towards the North. Soils in the North exhibit increased mineral salt content compared to those in the South. It is noteworthy that the samples are taken under identical conditions and at the same depth profile. In the field, the effectiveness of localized irrigation is

**Table 4.** Electrical conductivity and hydrogen potential measured from the soil solution at the upstream Tassaout

| Samples | Electrical conductivity (µS/cm) CE | Potential hydrogen pH |
|---|---|---|
| Aam | 66 | 7.93 |
| Bam | 112 | 7.82 |
| Cam | 173 | 7.57 |
| Dam | 177 | 7.66 |
| Eam | 227 | 7.75 |
| Fam | 160 | 7.72 |
| Gam | 199 | 7.83 |
| Ham | 345 | 7.65 |
| Iam | 140 | 8.38 |
| Jam | 295 | 7.72 |
| Kam | 160 | 7.63 |

**Table 5.** Electrical conductivity and hydrogen potential measured from the soil solution at the downstream Tassaout

| Samples | Electrical conductivity (µS/cm) | Potential hydrogen |
|---|---|---|
| Aav | 605 | 7.71 |
| Bav | 899 | 7.77 |
| Cav | 118 | 7.71 |
| Dav | 1 075 | 7.7 |
| Eav | 671 | 8.1 |
| Fav | 677 | 8.12 |
| Gav | 209 | 7.89 |
| Hav | 742 | 7.63 |
| Iav | 228 | 7.72 |
| Jav | 631 | 7.74 |
| Kav | 100 | 7.64 |

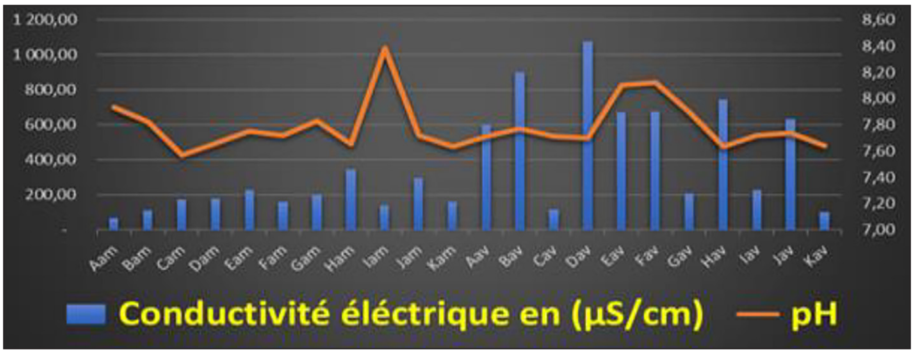


**Figure 12.** Electrical conductivity as a function of hydrogen potential at diagnostic sites

more pronounced in the upstream part of the Tassaout than in the downstream part. This observed change is attributable to soil leaching. The EC and pH data are combined and simplified in the following curve shown in Figure 12. The curve illustrates a relatively consistent variation between electrical conductivity (EC) and pH. When conductivity values decrease, we observe basic pH values, and in most cases, values close to neutrality. However, there is no significant difference in pH between upstream and downstream despite variations in EC.

## Texture and granulometric analysis

The following Table 6 presents the percentages of fractions in each sample according to the results of laser granulometry.

We proceed to represent the granulometric composition of these soil samples. We base this on the relative proportion of the three main granulometric fractions: sand, silt, and clay, using the USDA 1930 texture triangle diagram. The result of the corresponding laser granulometry for the upstream Tassaout is as shown in Figure 13.

**Table 6.** Percentages of clay, silt, and sand in soil samples

| Part | Samples | % Clays | % Stringers | % Sands |
|---|---|---|---|---|
| Tassaout amont | Aam | 20.31 | 65.3 | 14.39 |
| | Bam | 19.08 | 69.25 | 11.67 |
| | Cam | 14.22 | 70.66 | 15.12 |
| | Dam | 12.12 | 71.15 | 16.73 |
| | Eam | 14.99 | 67.41 | 17.6 |
| | Fam | 17.83 | 62.18 | 19.99 |
| | Gam | 13.93 | 63.16 | 22.91 |
| | Ham | 14.91 | 65.13 | 13.75 |
| | Iam | 17.7 | 68.55 | 13.75 |
| | Jam | 14.44 | 63.99 | 21.57 |
| | Kam | 17.18 | 63.15 | 19.67 |
| Tassaout aval | Aav | 10.24 | 56.39 | 33.37 |
| | Bav | 16.21 | 72.29 | 11.5 |
| | Cav | 13.81 | 60.68 | 25.51 |
| | Dav | 22.01 | 77 | 0 .99 |
| | Eav | 21.49 | 56.3 | 22.21 |
| | Fav | 21.01 | 66.37 | 12.62 |
| | Gav | 19.71 | 75.21 | 5.08 |
| | Hav | 16.21 | 63.88 | 19.91 |
| | Iav | -- | -- | -- |
| | Jav | 10.98 | 67.19 | 21.83 |
| | Kav | 9.71 | 65.42 | 24.87 |

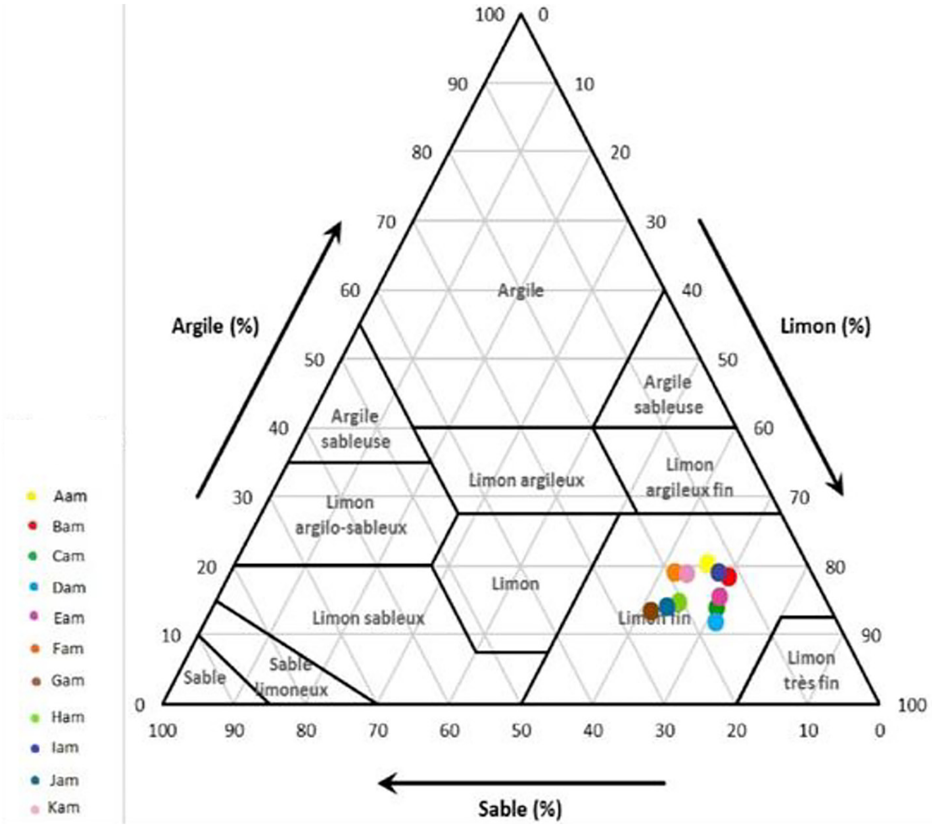


**Figure 13.** Triangular diagram representing the classes of samples from the upstream Tassaout

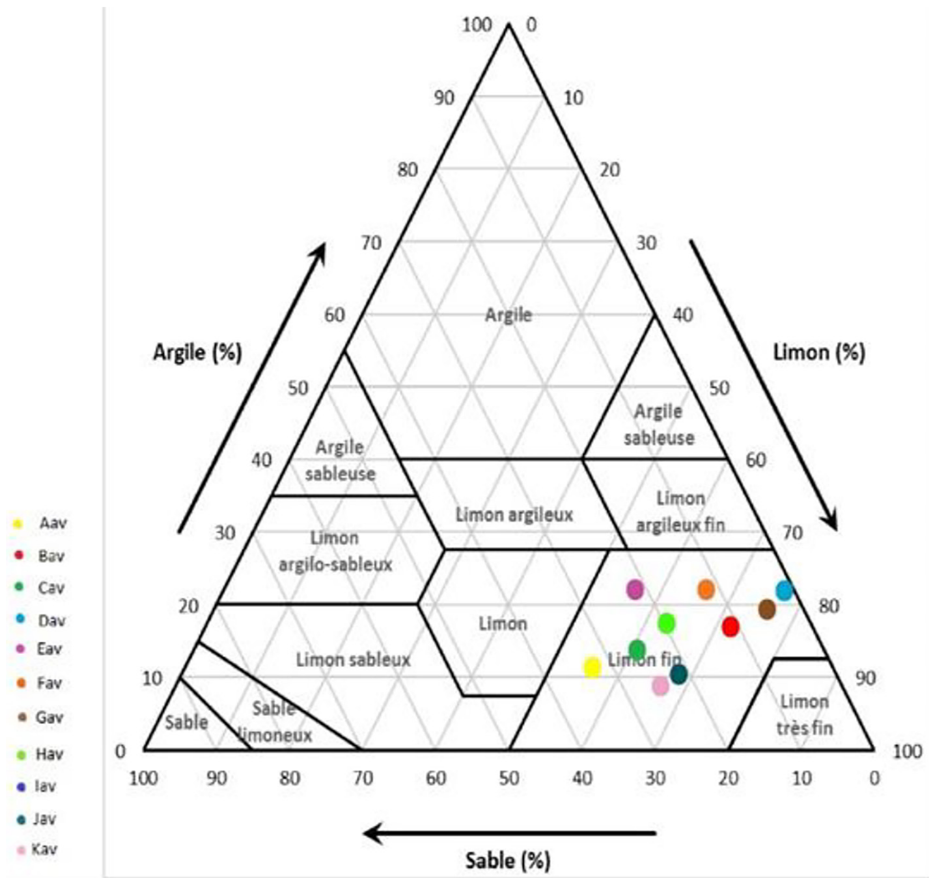


**Figure 14.** Triangular diagram representing the classes of samples from the downstream Tassaout

The result of the corresponding laser granulometry for the downstream Tassaout is as shown in Figure 14. The soils in the Tassaout region are primarily of a fine silty texture. This texture promotes higher agricultural yields and adequate water retention to meet the needs of crops. Silt particles facilitate water infiltration into the soil, thereby preventing waterlogging and stagnation issues, while promoting leaching and reducing surface mineral salt concentration. In this context, localized irrigation plays a crucial role in diluting the soil with appropriate and precise amounts of water.

## CONCLUSIONS

The results highlight favourable soil conditions in the upstream zone compared with the downstream zone, where low salinity coincides with greater mineralisation of organic matter and denser vegetation. The salinity indices were validated, and the interpolation maps showed consistency between the GIS data and the laboratory results. In summary, the study identified two distinct zones: an upstream zone with lower salinity and a downstream basin with higher salinity due to localised irrigation. Remote sensing predicted this divergence, which was confirmed by field analyses. Localised irrigation is more widespread upstream, which is attributed to its leaching effect, reducing the concentration of salt in the root zone and improving crop yields. Continued installation of the irrigation system requires regular biennial surveys to monitor trends in soil salinisation. Finally, this study, the first to be carried out in detail in this region, provides valuable information that will help farmers find future solutions and guide decision-makers in managing salinisation problems.

## REFERENCES

1. Al Droubi A., 1976. Géochimie des sels et des solutions concentrées par évaporation. Modèle thermodynamique de simulation. Application aux sols salés du Tchad. PhD Thesis, University of Strasbourg.
2. Roy A. C, 2008. Cartographie végétale du col de la vallée de Sverdrup, île d'Ellesmere, avec le NDVI MODIS et analyses des changements d'échelles". Mémoire, Université du Québec à Trois-Rivières, 86.
3. Annabi M., 2005. Stabilisation de la structure d'un sol limoneux par des apports de composts d'origine urbaine : relation avec les caractéristiques de leur matière organique, thèse à l'institut national agronome paris- grignon, 3.
4. Barbiéro L. and Vallès V. 1992. Aspects géochimiques de l'alcalinisation des sols dans la vallée du Dallol Bosso (République du Niger). Cah. Orstom, sér. Pédol., XXVII(2), 143152.
5. Barbiéro L. 1995. Les sols alcalinisés sur socle dans la vallée du fleuve Niger. Origine de l'alcalinisation et évolution des sols sous irrigation. Travaux et Documents Microfichés Orstom 138, 209.
6. Bellouti A., Cherkaoui, Benhida M., Debbarh A., Soudi B., Badraoui M. 2002. Mise en place d'un système de suivi et de surveillance de la qualité des eaux souterraines et des sols dans le périmètre irrigué du Tadla, au Maroc. Atelier du PCSI (Programme Commun Systèmes Irrigués) sur une Maîtrise des Impacts Environnementaux de l'Irrigation, Montpellier, France. 11.
7. Borgie M. 2014. Etude des particules fines et ultrafines en suspension dans l'air au Liban: caractérisation physicochimique et évaluation des effets toxicologiques sur des cellules pulmonaires humaines BEAS-2B. Thèse de doctorat, Université Libanaise Ecole Doctorale des Sciences et de Technologie (UL), 327.
8. Bradaï Abd., Douaoui Abd., Bettahar N., Yahiaoui I. 2016. Improving the Prediction Accuracy of Groundwater Salinity Mapping Using Indicator Kriging Method, J. Irrig. Drain Eng.
9. Cheverry C. 1974. Contribution à l'étude pédologique des polders du lac Tchad. Dynamique des sels en milieu continental subaride dans les sédiments argileux et organiques. Thèse. Science, U.L.P. Strasbourg, 257.
10. Derbbah A. and Badraoui M. 2003. Irrigation et environnement au Maroc: Situation actuelle et perspectives. In S. Marlet, P. Ruelle (eds), Vers une maîtrise des impacts environnementaux de l'irrigation. Cédérom du CIRAD, Montpellier, France Dervin Ch., 1992. Comment interpréter les résultats d'une analyse factorielle. Collection STAITCF. 93.
11. Michel F., Courard L. 2006. Apport de la granulométrie laser dans la caractérisation physique des fillers calcaires". Septième édition des Journées scientifiques du Regroupement francophone pour la recherche et la formation sur le béton (RF) 2B, GEMME - Matériaux de Construction, Département de Géoressources, Géotechnologies et Matériaux de Construction, Université de Liège, Belgique, 11.
12. Montoroi J.-P. 1997. Conductivité électrique de la solution du sol et d'extraits aqueux de sol application à un sol sulfaté acide salé de Basse-Casamance (Sénégal)". Étude et Gestion des Sols, Centre ORSTOM d'lle-de-France - Laboratoire des Formations Superficielles - 32, Avenue Henri Varagnat, 931 43 BONDY Cedex, 279–298.
13. Rochdane S., El Mandoura A., Amrhar M., Himi M.,

Casas A. 2012. Salinisation des eaux souterraines du Haouz oriental et du domaine de la Tassaout amont (Maroc occidental). Boletín Geológicoy Minero, 9.

14. Sadiki M., Markhi A., Elbelrhiti H., Mrabet S. 2016. Cartographie de la salinite à la surface du sol dans une zone du Prerif. cas de la region de l'Ouergha. European Scientific Journal, January Edition, 12(3), 197–223.
15. Samba R. 1998. Riziculture et dégradation des sols en vallée du fleuve Sénégal: analyse comparée des fonctionnements hydro-salins des sols du delta et de la moyenne vallée en simple et double riziculture. Thèse Doc. Ing., Uni. Cheikh Anta Diop de Dakar (Sénigal). 175.
16. SUHET, 2015. SENTINEL-2 User Handbook, ESA Standard Document, Agence spatiale européenne, 1(2), 64.
17. Vallès V., N'Diaye M.K., Bernadac A., Tardy Y. 1989. Mali. Al, Si and Mg in water concentrated by évaporation: development of a mode! Arid Soil Res. Rehabil. 3, 21–39.